JOURNAL OF PHYSICAL ORGANIC CHEMISTRY
J. Phys. Org. Chem. 2005; **18**: 864–869
Published online 6 June 2005 in Wiley InterScience (www.interscience.wiley.com). DOI: 10.1002/poc.955

Structural aspects of phase transition in pyrrole-2,5-dithioamide single crystals†

Lukasz Dobrzycki,[1] Tomasz Zielinski,[2] Janusz Jurczak[1,2] and Krzysztof Wozniak[1]*

[1]Department of Chemistry, Warsaw University, Pasteura 1, 02-093 Warszawa, Poland
[2]Institute of Organic Chemistry, Polish Academy of Sciences, Kasprzaka 44/52, 01-224 Warszawa, Poland

Received 13 December 2004; revised 11 April 2005; accepted 12 April 2005

ABSTRACT: The new pyrrole thioamide derivative 1*H*-pyrrole-2,5-dithiocarboxylic acid bis(*n*-butylamide) exists in two different phases with the first-order phase transition at ~195.8 K on heating up. We describe details of the lower and higher temperature phases and the nature of the phase transition. The high-temperature phase is centrosymmetric, with the molecule having one statically disordered aliphatic chain, whereas the low-temperature crystals are characterized by chiral $P2_1$ space group symmetry with the unit cell volume six times bigger than the volume of the high-temperature phase. Although the unit cell volume changes continuously with temperature, all other geometric parameters of the unit cell (a, b, c, β) change in a discrete manner during the phase transition. We propose a model explaining the structural disorder observed at high temperature and discuss the variation of properties of weak interactions on decrease of symmetry. Copyright © 2005 John Wiley & Sons, Ltd.

KEYWORDS: phase transition; static disorder; thiocarbonyl compounds; x-ray diffraction

INTRODUCTION

Among various areas in supramolecular chemistry, coordination of anions has been a subject of intensive exploring.[1] Development of neutral anion receptors is one of the most challenging tasks.[2] Our group has been interested in studies of macrocyclic effects, dependence between structure and binding abilities of ligands and in the invention of some new building blocks for receptors.[3] In the course of those studies we decided to investigate the thioamide group as the hydrogen bond donor.[4] We prepared pyrrole-2,5-dicarbothioamides as simple models for studying anion binding properties of the thioamides. Discussion of binding properties of this class of ligands will be published in a separate paper.

It appears that one of our model compounds—1*H*-pyrrole-2,5-dithiocarboxylic acid bis(*n*-butylamide) (Fig. 1)—undergoes a phase transition at 195.8 K and in this paper we describe the structures of both the low- and high-temperature phases as well as the details of structural changes during the phase transition. Polymorphism in molecular crystals and the transformation of one phase into another has focused significant attention.[5] In this paper we will concentrate on the structural aspects of the phase transition in the title compound.

**Correspondence to:* K. Wozniak, Department of Chemistry, Warsaw University, Pasteura 1, 02-093 Warszawa, Poland.
E-mail: kwozniak@chem.uw.edu.pl
†Selected paper presented for a special issue dedicated to Professor Otto Exner on the occasion of his 80th birthday.

EXPERIMENTAL

Synthesis of 1*H*-pyrrole-2,5-dithiocarboxylic acid bis(*n*-butylamide)

The monomethyl ester of 1*H*-pyrrole-2,5-dicarboxylic acid, obtained according to a literature procedure,[6] was hydrolysed to afford the appropriate diacid, which, after conversion into the corresponding acid dichloride, was subjected to reaction with butylamine. The resulting 1*H*-pyrrole-2,5-dicarboxylic acid bis(*n*-butylamide) was reacted with Lawesson's reagent to give 1*H*-pyrrole-2,5-dithiocarboxylic acid bis(*n*-butylamide) as yellow crystals in ~45% overall yield: m.p. 114–115 °C; ^{1}H NMR (200 MHz $CDCl_3$) $d = 10.529$ (s, 1H, N*H*-pyrrole), 7.380 (s, 2H, CSN*H*), 6.51 (d, 2H, $J_1 = 2.8$ Hz, *H*-pyrrole), 3.79 (dt, 4H, $J_1 = 7.4$ Hz, $J_2 = 5.6$ Hz, CH_2NH), 1.78–1.64 (m, 4H, CH_2), 1.52–1.34 (m, 4H, CH_2), 0.97 (t, 6H, $J_1 = 7.2$ Hz, CH_3); ^{13}C NMR (50 MHz $CDCl_3$) $d =$ 184.9, 134.6, 106.0, 45.5, 30.4, 20.2, 13.7; HR EI calc. for $C_{14}H_{23}N_3S_2$ M^+: 297.1333; found: 297.1332; Anal. calc. for $C_{14}H_{23}N_3S_2$: C 56.53, H 7.79, N 14.12, S 21.56; found: C 56.74, H 7.75, N 14.15, S 21.51. X-ray-quality crystals were obtained by slow diffusion of pentane into a dichloroethane solution of the thioamide.

Differential scanning calorimetry (DSC)

The DSC measurements were carried out on a Perkin-Elmer Pyris 1 compensatory microcalorimeter with a speed ratio of 10 °C min^{-1} at atmospheric pressure.

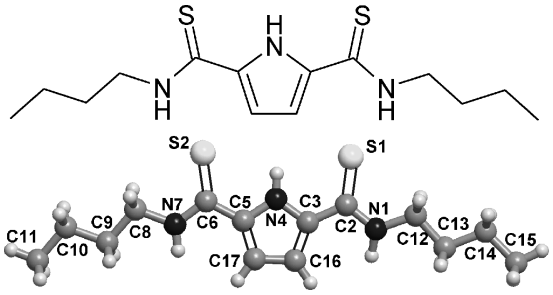

Figure 1. The $C_{14}H_{23}N_3S_2$ structural formula and labelling scheme for 1*H*-pyrrole-2,5-dithiocarboxylic acid bis(*n*-butylamide)

X-ray diffraction

The structure measurements were carried out on a single-crystal x-ray κ-axis KM4CCD diffractometer with graphite and monochromated Mo Kα radiation using the omega scan technique. For both experiments two different prismatic shaped single crystals were chosen: size $0.64 \times 0.49 \times 0.32\,mm^3$ for high-temperature (HT) measurement size $0.49 \times 0.34 \times 0.27\,mm^3$ for low-temperature (LT) measurement. The temperature was set at 200 K for the first measurement and at 120 K for the second measurement. In both cases the crystal was positioned 65 mm from the charge-coupled device (CCD) 1024×1024 pixel camera, and the same measurement scheme allowing acquisition of higher angle reflections was applied so that for both phases the 2θ angle range goes from $\sim 3°$ up to 70°. Each frame was measured with a 1° angle interval and counting times of 13 s (LT phase) and 15 s (HT phase) for the camera position at $2\theta = 30°$ and 26 s (LT phase) and 34 s (HT phase) for the camera position at $2\theta = 54°$. Data were corrected for Lorentzian and polarization effects. Due to the relatively low absorption coefficient ($\mu \sim 0.32\,mm^{-1}$), no absorption correction was applied. Data reduction and analysis were carried out with the Oxford Diffraction (Wroclaw) programs.[7]

Refinement details

Both structures were refined using data with maximum 2θ equal to 60° because of relatively weak higher angle reflection intensities. The data collection range gave 110 309 reflections collected and 55 909 unique reflections with $R_{int} = 3.1\%$ for the LT phase, with 2169 parameters. The HT phase is based on 4734 unique reflections (18 279 collected) with R_{int} equal to 2.6% and 268 parameters with six restraints. Limiting indices for the LT phase are $-38 \le h \le 38$, $-20 \le k \le 20$, $-38 \le l \le 38$ and for the HT phase are $-13 \le h \le 13$, $-20 \le k \le 20$, $-16 \le l \le 16$. Completeness of the data collection to $2\theta = 60°$ is 99.7% for the LT phase and 99.9% for the HT phase. The structures were solved by direct methods[8] and refined using SHELXL.[9] The refinements were based on F^2 for all reflections except those with very negative F^2. Weighted R factors wR_2 and all goodness-of-fit S values are based on F^2. Parameters R_1, wR_2 and S for the LT phase are 8.39%, 16.23% and 0.968, respectively, whereas for the HT phase they are 6.81%, 18.27% and 1.159, respectively. Conventional R_1 factors are based on F, with F set to zero for negative F^2. The $F_0^2 > 2\sigma(F_0^2)$ criterion was used only for calculating R factors and is not relevant to the choice of reflections for the refinement. Discrepancy factors for the $F_0^2 > 2\sigma(F_0^2)$ reflections are $R_1 = 0.0585$ and $wR_2 = 0.1437$ for the LT phase and $R_1 = 0.0601$ and $wR_2 = 0.1723$ for the HT phase. The R factors based on F^2 are about twice as large as those based on F. Scattering factors were taken from tables 6.1.1.4 and 4.2.4.2 in Ref. 10.

The extinction coefficient for both structures was not refined. The largest differential in electron density peak and hole are 1.072 eÅ^{-3} (0.06 Å from sulfur S1C atom) and -0.551 eÅ^{-3} for the LT phase and 0.665 eÅ^{-3} and -0.571 eÅ^{-3} for the HT phase, respectively. The Flack parameter[11] for the LT phase is 0.53(4).

RESULTS AND DISCUSSION

With increasing temperature the title compound has a phase transition at 195.8 K. Above that temperature it has a centrosymmetric, monoclinic space group $P2_1/n$ with one independent molecule with one disordered *n*-butyl chain and a unit cell volume of 1626 Å^3 [$T = 200(1)$ K; see Plate 1]. The LT phase has chiral space group $P2_1$ with 12 molecules in the independent part of the unit cell and 2169 refined parameters. The unit cell volume is 9619 Å^3 [$T = 120(1)$ K].

The phase transition passes rather rapidly with a distinct hysteresis. On cooling, the HT form persists down to 190.6 K, and on heating it is established at 195.8 K. A decrease of reflection intensities at the phase transition temperature is shown in Plate 2 (the middle picture).

The LT (120 K) phase unit cell parameters are $a = 27.140(5)$ Å, $b = 14.670(3)$ Å, $c = 27.171(5)$ Å and $\beta = 117.23(3)°$, whereas for the HT (200 K) phase they are $a = 9.785(1)$ Å, $b = 14.298(1)$ Å, $c = 11.817(1)$ Å and $\beta = 100.349(5)°$. The difference between the LT phase unit cell volume and the corresponding volume of six unit cells at HT is ~ 140 Å^3 (1.4%) for an 80 K interval and this seems to be a typical value for thermal expansion of molecular crystals.[12] Thermal expansion experiments show that the unit cell volume around the phase transition temperature changes linearly (see Fig. 2). A linear fit of V vs. T gives the following equation

$$V(T) = 9333(11) + 2.22(6) \times T, \quad \text{with } R = 0.997$$

A continuous change of the scaled unit cell volume between the LT and HT phases suggests that the phase

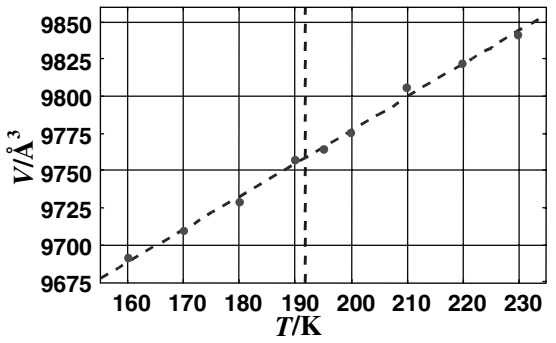

Figure 2. Unit cell volume (*V*) dependence on temperature (*T*)

transition is of the second-order type. It is interesting that all other geometrical parameters of the crystal (a, b, c, β) change in a discrete manner during the phase transition, which suggests the first-order type of transition. The dependences of the unit cell parameters on temperature in the range 160–230 K are shown in Fig. 3. To compare the unit cell parameters a, c and β, which are completely different for the two phases, one has to reorient and rescale the HT crystal lattice parameters to those for the LT phase using the following formulae

$$a_{\mathrm{LT}} = 2\sqrt{a_{\mathrm{HT}}^2 + c_{\mathrm{HT}}^2 + 2 \cdot a_{\mathrm{HT}} \cdot c_{\mathrm{HT}} \cdot \cos[\beta_{\mathrm{HT}}]}$$

$$c_{\mathrm{LT}} = \sqrt{a_{\mathrm{HT}}^2 + 4 \cdot c_{\mathrm{HT}}^2 - 4 \cdot a_{\mathrm{HT}} \cdot c_{\mathrm{HT}} \cdot \cos[\beta_{\mathrm{HT}}]}$$

$$\beta_{\mathrm{LT}} = \arccos\left(\frac{9 \cdot a_{\mathrm{HT}}^2 - a_{\mathrm{LT}}^2 - c_{\mathrm{LT}}^2}{2 \cdot a_{\mathrm{LT}} \cdot c_{\mathrm{LT}}}\right)$$

For the LT phase, a is almost constant around 27.12 Å and jumps up to 27.8 Å at the phase transition. Then, it decreases by ~0.1 Å with an increase of temperature up to 230 K. The most significant consequence of the phase transition for this parameter is its discrete jump of ~0.68 Å and a small negative expansion of the HT phase unit parameter.

The unique axis b in both phases does not require scaling and it changes discretely [~0.4 Å (2.8%)] at the phase transition temperature. For the HT phase the lowering of temperature is associated with a linear decrease of b down to the phase transition (230–192 K). Below it, b is almost constant (14.7 Å).

Parameter c changes similar to a. It slightly increases with temperature for the LT phase and then there is a small jump (~0.1 Å) on the phase transition and a small negative expansion for the HT phase.

The unique angle β decreases with increase of temperature, with a larger slope for the LT than for the HT phase. The parameter jump at the transition temperature is ~0.8°. It is interesting that discontinuous changes of all these unit cell parameters produce a linear dependence of the unit cell volume (V) on temperature, although in general for the monoclinic system the unit cell volume is a function of all of them: $V = a \times b \times c \times \sin(\beta)$. During the transition from HT to LT phase the area of the *ac* plane decreases, which is caused mainly by changes of β and a.

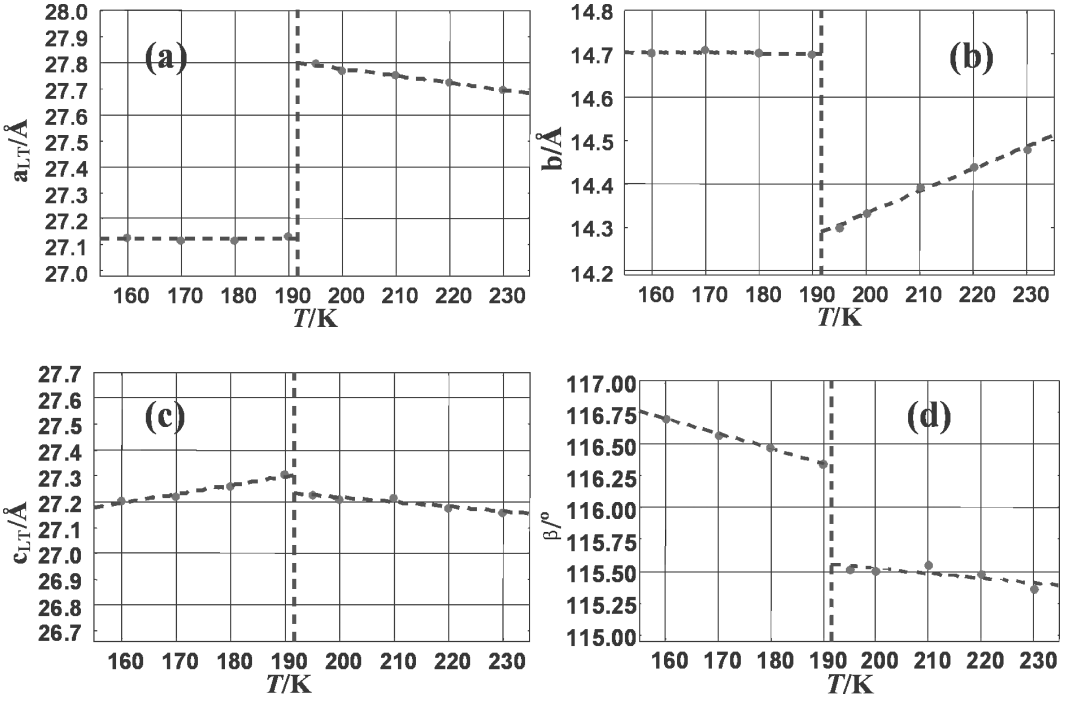

Figure 3. Dependences of the unit cell parameters vs. temperature: (a) *a* vs. *T*; (b) *b* vs. *T*; (c) *c* vs. *T*; (d) β vs. *T*

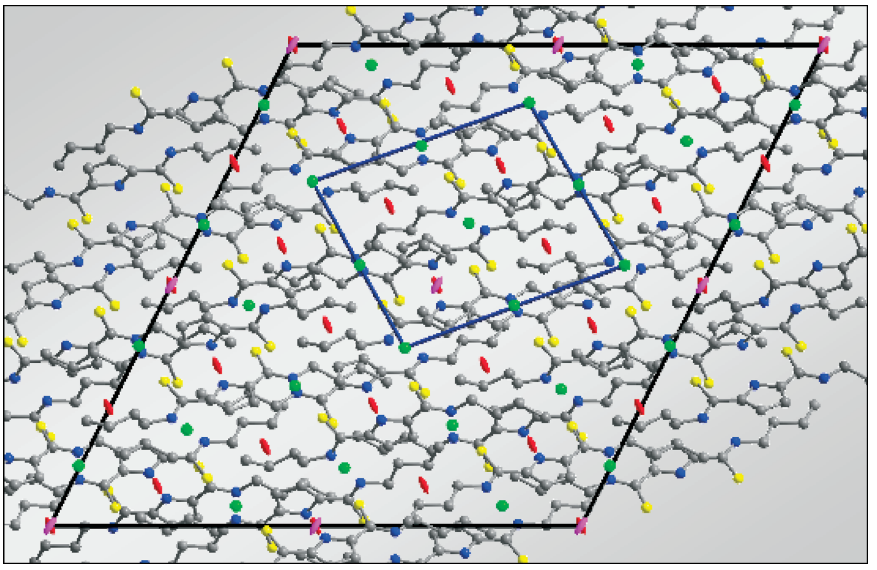

Plate 1. Relation between the shapes and sizes of the HT and LT unit cells, projected along the *Y*-axis. The HT unit cell is inside the bigger LT cell. The green dots are symmetry centres present in the HT crystal lattice. The red 2_1 screw axes are characteristic for the HT phase and the purple ones for the LT phase

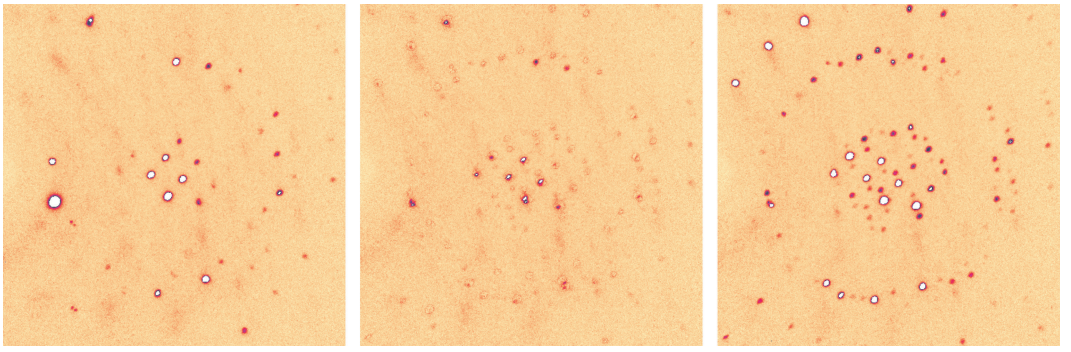

Plate 2. Manifestation of the phase transition in the reciprocal crystal lattice plane (*X**0*Z**) view along the *Y*-direction arranged towards the detector: the HT phase at $T = 200$ K (left); the LT phase at $T = 190$ K (right); during the phase transition at averaged $T = 193$ K (middle)

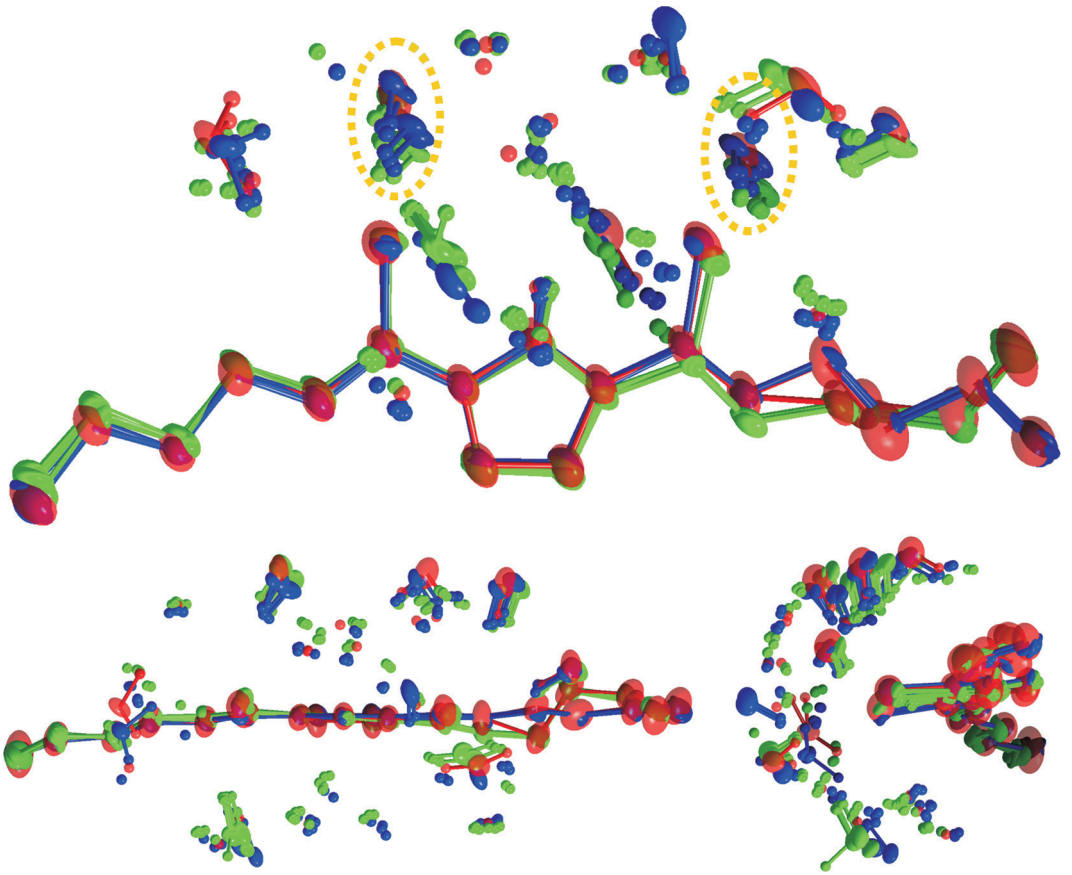

Plate 3. Three projections of superposition of all LT and one HT independent molecules, including their closest environments. The HT molecule is red, the six LT symmetric molecules are blue and the LT asymmetric molecules are green. The donating N—H groups interacting with sulfur atoms are marked by dashed, orange ellipsoids. The probability level for all ADPs is 50%

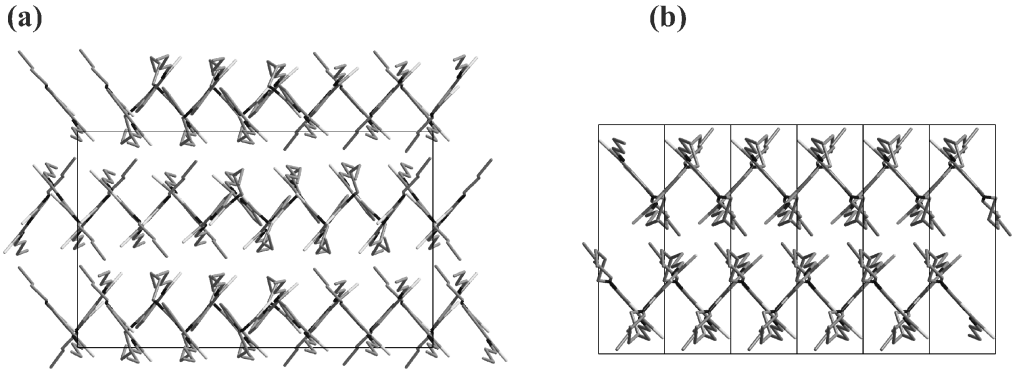

Figure 4. The LT (a) and HT (b) unit cells projected along the [100] and [$\bar{1}$02] directions, respectively

Comparison of the results for the LT and HT data sets shows that the level of refinement for both structures is comparable in spite of the considerably larger number of refined parameters for the LT phase (2169 and 269 parameters for the LT and HT crystals, respectively). In both cases the ratio of the number of unique reflections to parameters is high (25.8 for the LT and 17.6 for the HT phase).

Lowering of the symmetry of a structure increases the number of independent reflections, so the ratio of the unique reflections to parameters should not change much. However, for this compound—because of disorder at higher temperature—some atoms occupy two positions, thus increasing the number of refined parameters, which is why this ratio is worse than that for the LT phase (despite the fact that there are 12 independent molecules in the LT unit cell).

The centrosymmetric crystal lattice of the HT phase is built from disordered averaged molecules. Although we tried to refine this structure using a bigger unit cell or changing its symmetry to resolve disorder, we failed. At low temperature the crystal lattice changes into a chiral structure that is in fact a 'racemic twin', with the Flack parameter $\sim$0.5. Apparently, the unit cell of the LT phase is chiral but the whole crystal is a racemate consisting of chiral domains. The phase transition starts simply at the same time at different positions, probably from defects, and it is unlikely that this process prefers one of the two possible options.

Plate 1 explains why the LT phase, in contrast to the HT phase, is not centrosymmetric. The unit cell reorientation during the transitions from HT to LT phase results in dropping the centres of symmetry $\bar{1}$, the glide plane n or the 2_1 screw axes. In consequence, this decreases the symmetry to either triclinic space group $P\bar{1}$ or a chiral monoclinic space group $P2_1$ (with the unit cell origin at 2_1—the pink axes). The $P2_1/m$ group is forbidden. Comparison of structure refinement parameters in the above space groups finally confirmed the $P2_1$ space group (considerably lower discrepancy factors, physically sensible thermal ellipsoids of all atoms and lack of disorder). Apparently, at low temperature the difference between less vibrating molecules becomes far more significant.

Plate 1 shows that the closest environment of the HT inversion centres differs for the LT phase. Of course, at higher temperatures the higher thermal motion of all molecules is averaging out these small differences, which increases the symmetry of this phase. The unit cell b parameter change on the phase transition seems to be the most significant for the lowering of the symmetry of the system. Comparison of unit cell views perpendicular to the x-direction is shown in Fig. 4.

The HT phase unit cell contains 4×1 molecules whereas the LT phase unit cell contains 2×12 molecules. So, during the transition from LT to HT phase 12 molecules from the LT unit cell are averaged out, giving one statically disordered molecule at high temperature. Thermal motion analysis seems to confirm such a process. Figure 5 shows thermal ellipsoids of all superimposed molecules at low temperature (a,b) and

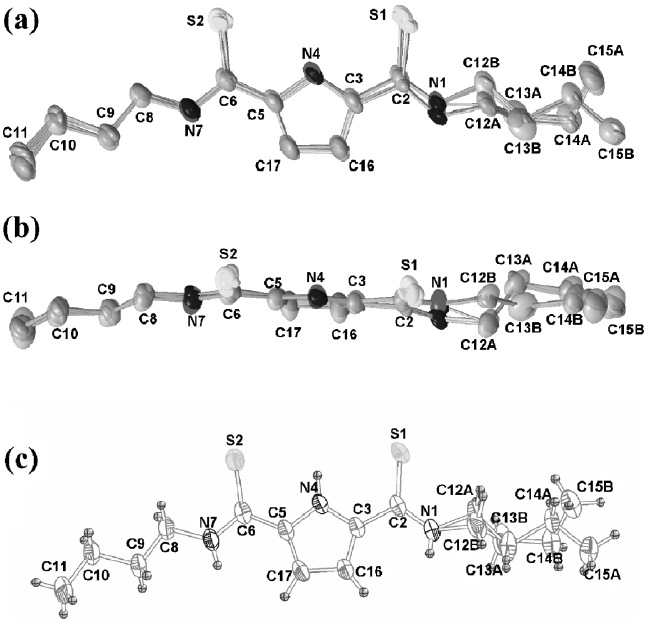

Figure 5. Comparison of thermal ellipsoids obtained for atoms of molecules in LT and HT phases: (a,b) projections of thermal ellipsoids of superimposed LT moieties; (c) ADPs of the HT independent molecule. For all ADPs, the probability level is 50%

Table 1. Details of N—H . . . S hydrogen bonds formed in both phases

D—H donor	A acceptor	Symmetry	*d*(D—H) (Å)	*d*(H . . . A) (Å)	*d*(D . . . A) (Å)	<DHA°
LT phase						
N7L-H7L	S1A	[$x-1$,y,z]	0.88	2.59	3.456(3)	168.4
N1G-H1G	S2A		0.92(4)	2.61(4)	3.511(3)	166(3)
N7G-H7G	S1B		0.89(3)	2.60(3)	3.481(3)	167(3)
N1H-H1H	S2B		0.95(3)	2.63(3)	3.558(3)	169(3)
N7H-H7H	S1C		0.93(3)	2.56(3)	3.475(3)	167(3)
N7K-H7K	S2C	[$-x+1$,$y-1/2$,$-z+2$]	0.79(4)	2.85(4)	3.629(3)	170(4)
N7I-H7I	S1D		0.88	2.69	3.548(3)	166.0
N1L-H1L	S2D	[$-x+1$,y$+1/2$,$-z+1$]	0.79(4)	2.62(4)	3.347(3)	154(3)
N7J-H7J	S1E		0.88	2.71	3.567(3)	166.7
N1I-H1I	S2E		0.81(4)	2.68(4)	3.420(4)	154(4)
N1J-H1J	S1F		0.88(4)	2.62(4)	3.461(3)	162(4)
N1K-H1K	S2F	[$x+1$,y,z]	0.91(3)	2.72(4)	3.589(3)	160(3)
N7C-H7C	S1G	[$x-1$,y,z]	0.83(5)	2.70(5)	3.496(3)	160(4)
N7F-H7F	S2G	[$-x+1$,$y-1/2$,$-z+2$]	0.88	2.75	3.602(3)	163.1
N1F-H1F	S1H	[$-x+1$,$y-1/2$,$-z+2$]	0.86(5)	2.75(5)	3.560(3)	159(4)
N1E-H1E	S2H	[$-x+1$,$y-1/2$,$-z+2$]	0.88	2.60	3.416(3)	155.2
N7A-H7A	S1I	[$-x+1$,$y+1/2$,$-z+1$]	0.84(3)	2.64(4)	3.480(3)	172(3)
N1B-H1B	S2I	[$-x+1$,$y+1/2$,$-z+1$]	0.88	2.71	3.549(3)	159.9
N7D-H7D	S1J	[$x+1$,y,z]	0.95(4)	2.63(4)	3.566(3)	170(3)
N1A-H1A	S2J	[$-x+1$,$y+1/2$,$-z+1$]	0.88	2.56	3.369(3)	153.9
N1D-H1D	S1K		0.88	2.61	3.437(3)	156.2
N7E-H7E	S2K		0.91(5)	2.71(5)	3.616(3)	172(4)
N7B-H7B	S1L		0.97(4)	2.47(4)	3.438(3)	174(3)
N1C-H1C	S2L		0.91(3)	2.71(3)	3.530(3)	150(2)
HT phase						
N7-H7	S1	[$x-1/2$,$-y+1/2$,$z+1/2$]	0.83(3)	2.73(3)	3.544(2)	165(2)
N1-H1	S2	[$x-1/2$,$-y+1/2$,$z-1/2$]	0.80(3)	2.89(3)	3.680(2)	170(2)

comparison of these with the HT thermal motions of atoms (c). All LT and HT phase molecules have been superimposed using the least-squares method (all equivalent non-hydrogen atoms from each moiety were fitted one to another) and there seems to be quite good agreement between these figures. The proposed model explains the non-physical direction of Atomic Displacement Parameters of heavy atoms at high temperature and their elongation along the S—C bonds.

There are some interesting weak interactions present in both structures (see Table 1) that are responsible for the three-dimensional ordering of molecules in the crystal lattice. These are mainly N—H . . . S hydrogen bonds, but accompanied by relatively short S . . . H—C and C . . . H—N intermolecular contacts slightly more distant than the sum of van der Waals' radii of the interacting atoms. Because these weak hydrogen bonds have electrostatic nature they may influence the structure even beyond the van der Waals' limit. These interactions are the most flexible and differentiate easily on decrease of temperature. As is common for such space groups, the three-dimensional crystal lattice is formed by molecules oriented differently in the neighbouring layers in order to facilitate numerous weak interactions.

Because each sulfur atom forms an N—H . . . S hydrogen bond, one can examine the differences between the hydrogen bonds formed by different sulfur atoms in one moiety. When the difference between the S . . . H distances in the HT form is taken as a reference system (red data points in Fig. 6), it appears that on cooling such a difference between hydrogen bonds formed by two sulfur atoms in one moiety increases for six molecules in the LT form and decreases for the rest of the moieties. These are good examples of rearrangement of molecules in the crystal lattice on cooling. Changes of weak interactions are well illustrated in Plate 3, which is a superposition of

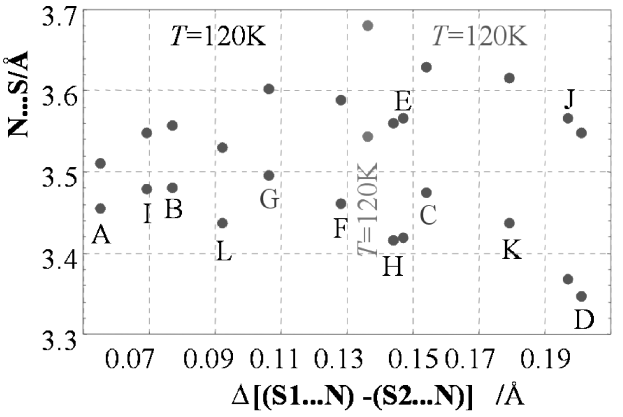

Figure 6. Donor—acceptor interatomic S . . . N distances for hydrogen bonds formed by both sulfur atoms in each independent moiety of the LT and HT (red data points) phases as a function of difference (Δ[(S1 . . . N) $-$(S2 . . . N)]) between the S . . . N distances. Capital letters denote particular moieties

all LT independent molecules, including their closest environments. The donating N—H groups are in the orange ellipsoids.

In conclusion, for the two (HT and LT) phases of 1*H*-pyrrole-2,5-dithiocarboxylic acid bis(*n*-butylamide) the temperature of the phase transition is 195.8 K on heating. This is the first-order type of phase transition with a distinct hysteresis. The relation between the two phases involves the formation of a racemic twin in the LT form. Although changes of the unit cell parameters vs. temperature lead to a smooth change in the unit cell volume, particular unit cell parameters change in a discrete manner. We propose a model explaining both the structural disorder observed at high temperature and the variation of properties of weak interactions on decrease of symmetry.

Acknowledgement

The x-ray measurements were undertaken in the Crystallographic Unit of the Physical Chemistry Laboratory at the Chemistry Department of the University of Warsaw.

REFERENCES

1. (a) Gale PA. *Coord. Chem. Rev.* 2003; **240**: 191–221; (b) Schmidtchen FP, Berger M. *Chem. Rev.* 1997; **97**: 1609–1646.
2. Bondy CR, Loeb S. *Coord. Chem. Rev.* 2003; **240**: 77–99.
3. (a) Szumna A, Jurczak J. *Eur. J. Org. Chem.* 2001; 4031–4039; (b) Chmielewski MJ, Jurczak J. *Tetrahedron Lett.* 2004; **45**: 6007–6010; (c) Chmielewski MJ, Charon M, Jurczak J. *Org. Lett.* 2004; **6**: 3501–3504.
4. (a) Lee H-J, Choi Y-S, Lee K-B, Park J, Yoon C-J. *J. Phys. Chem.* 2002; **A106**: 7010–7017; (b) Allen FH, Bird CM, Rowland RS, Raithby PR. *Acta Crystallogr.* 1997; **B53**: 680–695.
5. (a) Dunitz JD, Bernstein J. *Acc. Chem. Res.* 1995; **28**: 193; (b) Gavezzotti A. *Acc. Chem. Res.* 1994; **27**: 399; (c) Mnyukh Y. *Fundamentals of Solid-State Phase Transitions, Ferromagnetism and Ferroelectricity.* 1st Book Lib.: Bloomington, UK, 2001; (d) Bernstein J. *Polymorphism In Molecular Crystals*. Clarendon Press: Oxford, UK, 2002.
6. Barker P, Gendler P, Rapoport H. *J. Org. Chem.* 1978; **43**: 4849–4855.
7. Oxford Diffraction. *CrysAlis CCD and CrysAlis RED*. Oxford Diffraction: Wroclaw, Poland, 2001.
8. Sheldrick GM. *Acta Crystallogr.* 1990; **A46**: 467–473.
9. Sheldrick GM. *SHELXL97. Program for the Refinement of Crystal Structures.* University of Göttingen: Germany, 1997.
10. Wilson AJC. *International Tables for Crystallography*, vol. C, Kluwer: Dordrecht, 1992.
11. Flack HD. *Acta Crystallogr.* 1983; **B39**: 876–881.
12. Kitaigorodskii AI. *Molecular Crystals and Molecules*. Academic Press: New York, 1973.